

Synthesis, Characterization, and Properties of Homopolymers Functionalized with Oligothiophene Derivatives in the Side Chain

Chunchang Zhao,[†] Yong Zhang,[‡] Shanlin Pan,[†] Lewis Rothberg,^{†,‡} and Man-Kit Ng^{*,†}

Department of Chemistry and Department of Chemical Engineering, University of Rochester, Rochester, New York 14627

Received October 4, 2006; Revised Manuscript Received January 2, 2007

ABSTRACT: Two novel polynorbornenes **11** and **12** functionalized with electronically active conjugated oligomer units in the side chain were synthesized by the ring-opening metathesis polymerization (ROMP) method. Both polymers showed good optical characteristics, thermal stability, film-forming properties, and interesting electrochemical properties. The photophysical and redox behaviors of **11** and **12** are markedly different due to variation in the structure of the pendant oligomers. Polymer **11** with phenyl end-capped oligothiophene co-oligomer in the side chain showed much higher stability toward electrochemical oxidation than **12** with a sexithiophene in the side chain. This was demonstrated by in-situ study of the changes in absorption spectra of the polymer films while varying the potential in electrochemical experiments. During the p-doping process, polymer **11** exhibited highly reversible changes in its absorption peaks when monitored at 430 and 650 nm, and the p-doping/dedoping processes can be repeated many cycles. In sharp contrast, polymer **12** was shown to be electrochemically unstable under the same conditions. Single-layer photovoltaic cells have been fabricated with **11** or **12** as the active organic layer, and their relative performances were compared. These single-layer devices showed relatively large open-circuit voltage and moderate short-circuit current. In addition, the solar cell fabricated from **11** showed better device stability under ambient conditions than that from **12**, which can be attributed to the higher stability of phenyl end-capped oligothiophene co-oligomer compared to that of the sexithiophene.

Introduction

Thiophene-based π -conjugated oligomers and polymers have been the subject of intense study in the past two decades due to their potential applications in many fields such as field effect transistors, photovoltaic cells, charge-transporting materials, and nonlinear optical materials.^{1,2} High-performance electron- or hole-transporting materials that exhibit relatively high charge carrier mobilities have been identified. One current challenge facing organic semiconducting materials in practical applications is their stability issues under ambient conditions. Since most of the p-channel organic semiconductors have relatively high-lying highest-occupied molecular orbital (HOMO) level and small band gaps, they tend to be particularly labile toward photochemically and/or thermally induced oxidation processes, resulting in fast degradation, decreased device efficiency, and shortened lifetime for these organic devices. One way to avoid these undesirable effects is to lower the HOMO level of the semiconducting materials in order to prevent them from undergoing photoinduced or thermally induced oxidation reactions, thereby improving their environmental stability. A number of materials designs have been explored to test this hypothesis, including reduction of effective conjugation length of π -conjugated polymers in order to inhibit electronic delocalization along backbone,³ incorporation of electron-withdrawing substituents to polymers,⁴ and more recently end-capping the terminal α,ω -positions of oligothiophenes with chemically and electrochemically stable substituents.^{5–7} A more recent approach involves using polymers with stable backbone by incorporation of environmentally stable conjugated oligomers in the side chain.⁸ The incorporation of electronically active conjugated oligomers into polymer structures essentially combines the

properties of the specific oligomer with the desirable properties of polymer such as mechanical strength and film-forming properties, and this approach is desirable for practical device application. A few reports^{8–10} have showed that oligothiophenes can be attached to polymers as side chains, and the resulting materials exhibited electrical conductivity in the range of semiconductors and have potential applications in electrochromic devices. Polymers containing π -conjugated oligomers in the side chain are therefore of particular interest because of the wide variety of oligomers available, processability, supramolecular self-assembly properties attainable by the appropriate choice of side group, and potential applications in electronic devices.^{9,10} We have recently reported a new polynorbornene system with phenyl end-capped oligothiophene co-oligomer unit in the side chain.⁸ The polymer showed good photophysical characteristics, thermal stability, and film-forming properties. More importantly, a single-layer photovoltaic cell fabricated from this polymer showed relatively large open-circuit voltage ($V_{OC} = 0.7$ V), moderate short-circuit current ($I_{SC} = 0.7 \mu A/cm^2$), and excellent device stability under ambient conditions. We herein reported the detailed synthesis of two structurally related polymers with their structures optimized by elongating the spacer length between the polymer backbone and the co-oligomer unit. These two polymers differ only in the structure of the corresponding oligothiophene units in the side chains (one with while the other without phenyl end-capping groups). The optical, electrochemical, and photovoltaic properties of these polymer systems have been investigated, and their differences in performance are mainly caused by the higher electrochemical stability of the polymer with end-capping phenyl substituent.

Results and Discussion

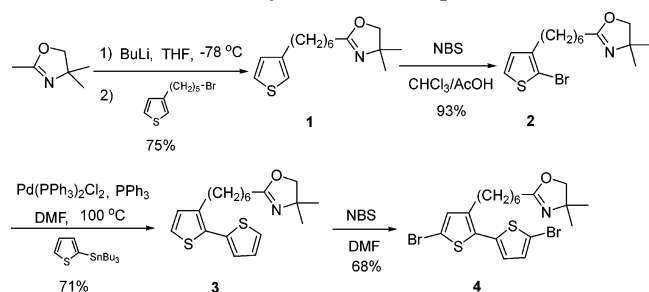
Synthesis of Monomers and Polymers. The synthesis of monomers and polymers are depicted in Schemes 1–3. The key intermediate dibromobithiophene (**4**) was obtained in four steps

* Corresponding author. E-mail: ng@chem.rochester.edu.

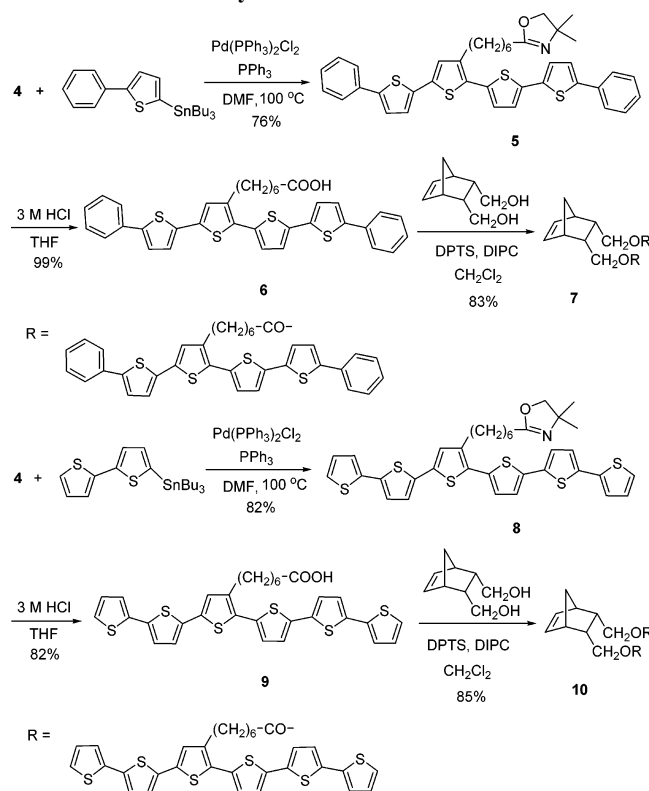
[†] Department of Chemistry.

[‡] Department of Chemical Engineering.

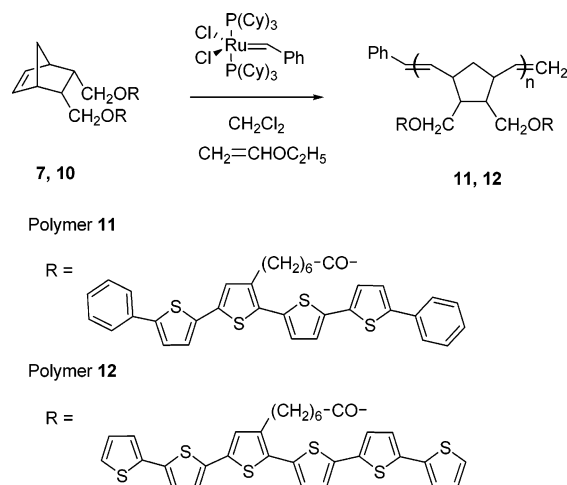
Scheme 1. Synthesis of Bithiophene 4



Scheme 2. Synthesis of Monomers 7 and 10



Scheme 3. Ring-Opening Metathesis Polymerization of Monomers 7 and 10



starting from 3-(5-bromopentyl)thiophene by known methods including displacement of bromide with anion of oxazoline, regioselective bromination,¹¹ and a palladium-catalyzed Stille cross-coupling.¹² The intermediate **4** was subject to additional Stille coupling with 2-(tributylstannyl)-5-phenylthiophene or

5-(tributylstannyl)-2,2'-bithiophene to afford **5** and **8** in 76% and 82% yield, respectively. Treatment of a suspension of **5** or **8** in THF with 3 M hydrochloric acid gave the corresponding acid **6** or **9**. The reaction of acid **6** or **9** with 5-norbornene-*endo*-2,3-dimethanol in the presence of *N,N'*-diisopropylcarbodiimide (DIPC) and *p*-(dimethylamino)pyridinium *p*-toluenesulfonate (DPTS) afforded the monomers **7** and **10** in good yields.

The two monomers (**7** or **10**) were separately polymerized by using the ring-opening metathesis polymerization (ROMP) method, as shown in Scheme 3. The polymerization was performed with commercially available bis(tricyclohexylphosphine)benzylidene ruthenium(IV) dichloride (first generation Grubbs' catalyst) as initiator in dry CH_2Cl_2 under nitrogen.¹³ The polymerization was allowed to run for 22 h under reflux, during which time the precipitate appeared, and then terminated by quenching with excess ethyl vinyl ether. The polymers were readily obtained in pure form by filtration of the precipitate followed by washing with CH_2Cl_2 for the removal of catalyst and any unreacted monomers. The molecular weights of the polymers were determined by gel permeation chromatography (GPC), using THF as the eluent and polystyrene as the standard. The molecular weight (M_w) was determined to be 14 900, and polydispersity was 1.21 for polymer **11**. The corresponding M_w and PDI values for polymer **12** were 32 700 and 1.23, respectively.

Thermal Properties. The thermal properties of polymers **11** and **12** were evaluated by means of thermogravimetric analysis (TGA) and differential scanning calorimetry (DSC) under a nitrogen atmosphere, and the results are summarized in Table 1. It is apparent that both polymers exhibited excellent thermal stability as the decomposition temperature for 5% weight loss were found to be 386 and 388 °C for **11** and **12**, respectively. The glass transition temperatures (T_g) were determined to be 83.1 and 71.7 °C for **11** and **12**, respectively.

Optical Properties. The UV-vis absorption and emission spectra of various monomers and polymers in *o*-dichlorobenzene and as thin films were recorded at room temperature and are shown in Figures 1 and 2. In the present polymer systems, a flexible alkyl spacer has been introduced to separate each of the side-chain oligothiophene unit from the polynorbornene backbone. In good agreement with what we have observed previously for the absorption behavior of a structurally related system,⁸ the absorption maximum (λ_{max}) of polymer **11** (421 nm) is only slightly blue-shifted in comparison with that of monomer **7** (426 nm), while the λ_{max} for polymer **12** (432 nm) remains virtually unchanged when compared to monomer **10** (432 nm). On the other hand, the emission maxima for both polymers are significantly red-shifted compared with their respective monomers. The emission maxima of polymer **11** (558, 592 nm) are bathochromically shifted by ~51 nm, and its emission bands retain part of the structured features when compared to those of monomer **7** (517, 541 nm). The λ_{max} for the emission of polymer **12** is centered at 586 nm, and the emission band has become somewhat broadened and structureless, in contrast to those of monomer **10** which are located at 525 and 559 nm together with a more well-defined structure.

Figure 2 compares the UV-vis absorption and emission spectra of polymers **11** and **12** in solutions and as thin films, which were prepared by spin-coating onto glass slides from *o*-dichlorobenzene. The absorption maxima of **11** and **12** in solution are at around 421 and 432 nm, respectively, while their thin films are bathochromically shifted to 432 and 441 nm, respectively. It is noteworthy that the absorption spectra of these

Table 1. Selected Properties of Polymers 11 and 12

polymer	M_w^a	PDI	T_d^b (°C)	T_g (°C)	E_1^c (V vs Fc/Fc ⁺)	E_2^c (V vs Fc/Fc ⁺)	solution ^d		film	
							λ_{\max} (nm)	λ_{em} (nm)	λ_{\max} (nm)	λ_{em} (nm)
11	1.5×10^4	1.21	386	83.1	0.87	0.49	421	558, 592	432	560, 595
12	3.3×10^4	1.23	388	71.7			432	586	441	587

^a Weight-averaged molecular weight. ^b Decomposition temperature based on 5% weight loss. ^c Measured in acetonitrile containing 0.01 M Bu₄NPF₆. A Pt electrode coated with a thin polymer film was used as the working electrode. ^d Measured in *o*-dichlorobenzene.

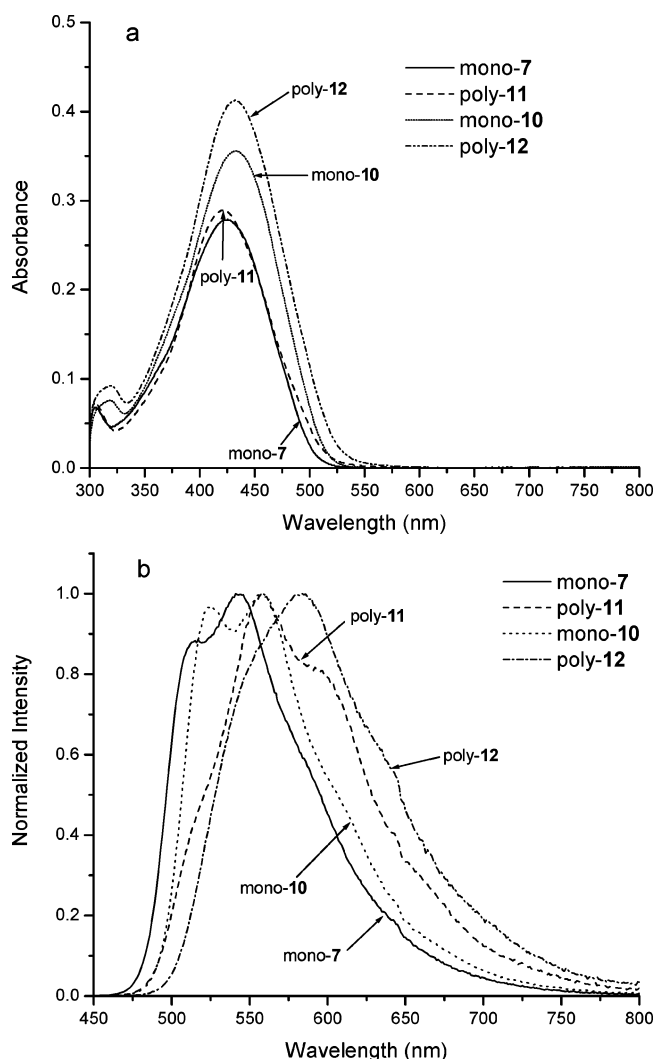


Figure 1. (a) UV-vis absorption spectra of monomers **7**, **10** (**7**: $\epsilon_{\max} = 6.2 \times 10^4 \text{ M}^{-1} \text{ cm}^{-1}$, **10**: $\epsilon_{\max} = 7.9 \times 10^4 \text{ M}^{-1} \text{ cm}^{-1}$) and polymers **11**, **12** ($c = 0.006 \text{ mg/mL}$) in *o*-dichlorobenzene. (b) Normalized emission spectra of the same monomers and polymers in *o*-dichlorobenzene.

thin films have been well extended into the neighborhood of 700 nm (Figure 2a), suggesting an enhanced absorption efficiency of these solid films in the long-wavelength region. On the other hand, the emission maxima of polymer thin films are not much different from those in solutions (Table 1), except that the emission bands in the solid state tend to be extensively broadened (Figure 2b). The red-shifting and band-broadening effect are presumably the result of slightly increased π - π stacking interactions in the solid state, a phenomenon commonly observed in conjugated polymers.

Electrochemical Properties. The redox properties of polymers **11** and **12** were investigated by cyclic voltammetric (CV) experiments, which were performed in acetonitrile containing Bu₄NPF₆ as supporting electrolyte at a scan rate of 100 mV/s at room temperature. A platinum electrode coated with a thin polymer film was used as the working electrode. A gold disk

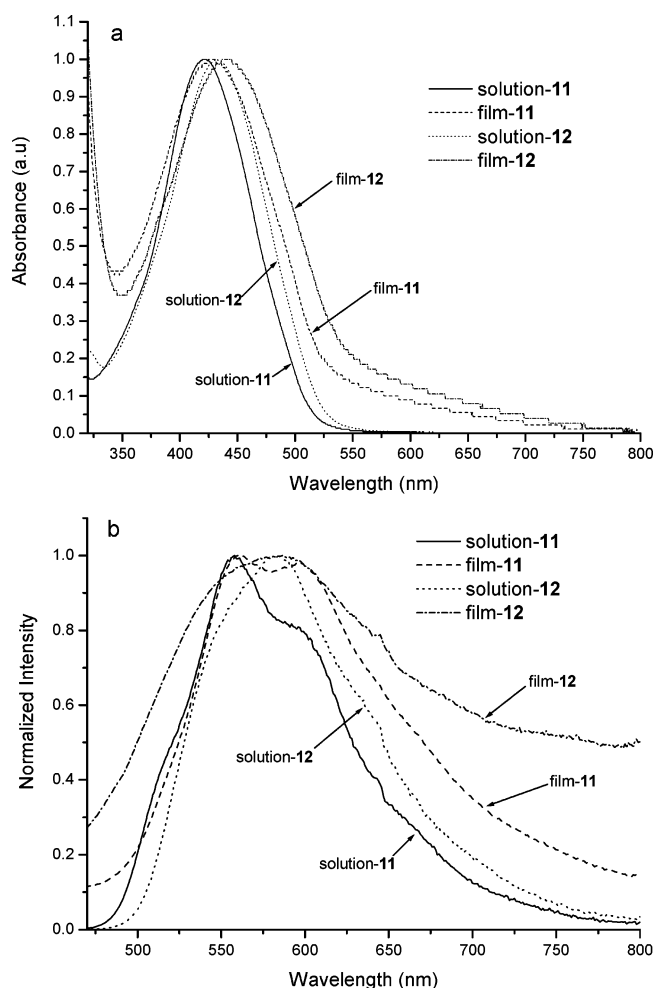


Figure 2. (a) Normalized UV-vis absorption of polymers in *o*-dichlorobenzene and as thin films. (b) Normalized emission spectra of polymers in *o*-dichlorobenzene and as thin films.

was used as the counter electrode, and Ag/AgNO₃ was used as the reference electrode. All reported potentials are calibrated against the ferrocene/ferrocenium (Fc/Fc⁺) couple, which was used as the internal standard. The resulting cyclic voltammograms showing four consecutive scan cycles are outlined in Figure 3 for each polymer. In both cases, the electrochemical responses of the oligothiophene-functionalized polymers became stabilized immediately after the initial cycle. Beginning from the second scan cycle, the voltammograms remained more or less unchanged for both polymers. The redox behaviors of **11** and **12** are vastly different due to different end-group substitution on the pendant oligomer unit. Polymer **11** clearly displayed two quasi-reversible oxidation processes with half-wave potentials at about 0.49 and 0.87 V (Figure 3a). In contrast, polymer **12** showed one significant anodic peak (E_{pa}) at 0.83 V during the initial anodic scan (Figure 3b), suggesting that a major oxidative process may be responsible. Upon reversal to cathodic direction, a reduction peak (E_{pc}) could be observed at ca. 0.32 V, which

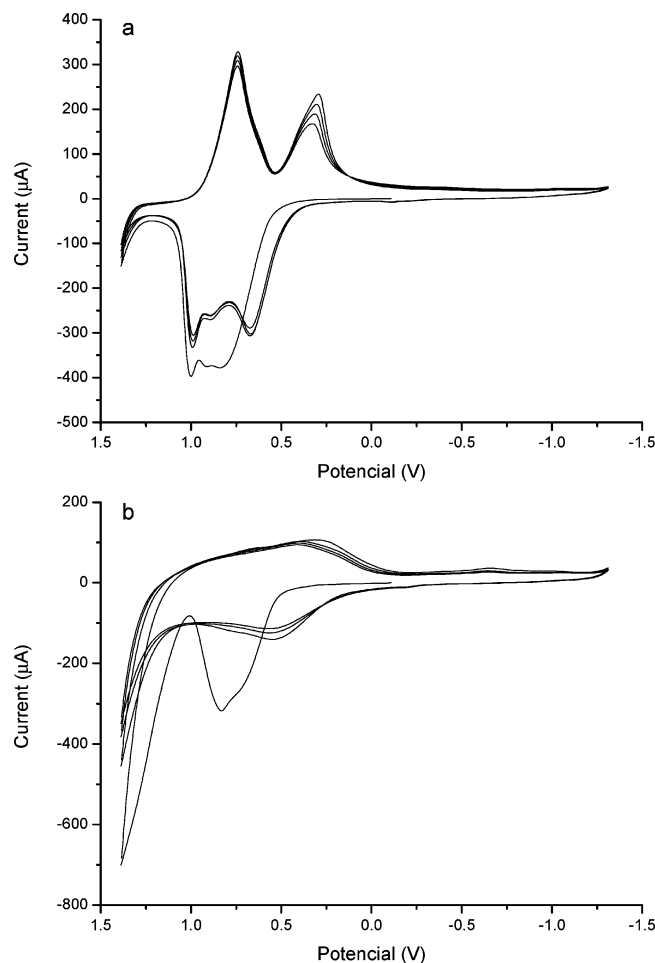


Figure 3. Cyclic voltammograms of polymer films of (a) **11** and (b) **12** coated on platinum plate working electrodes performed in acetonitrile containing Bu_4NPF_6 (0.01 M) as supporting electrolyte at room temperature, with a scan rate 100 mV/s. Potentials are versus the ferrocene/ferrocenium (Fc/Fc^+) couple.

can be attributed to the reduction of cross-linked polymer resulting from electrochemical polymerization of the sexithiophene side chain present in **12**.^{14,15} Upon a second scan cycle, a new oxidation process occurred at ~ 0.55 V (E_{pa}), which can be attributed to the oxidation of a newly in-situ formed cross-linked conjugated polythiophene backbone within polymer **12**. Scanning in the reverse direction led to a cathodic process with a response identical to that observed in the initial scan. Upon repeated cycling up to the fourth cycle, no further change in electrochemical response could be observed. These observations strongly indicate that oxidative coupling among the electron-rich oligothiophene units in **12** has taken place, and this process was essentially completed after the initial oxidative cycle. Tentatively, we believe the various cyclic voltammograms obtained upon repeated cycling as shown in Figure 3b all correspond to the same cross-linked polymeric structure derived from **12**. It is apparent that polymer **11** end-capped with phenyl substituents at the terminal positions of the oligothiophene has prevented such an undesirable oxidative polymerization from taking place and is therefore electrochemically more stable than polymer **12** without such phenyl protecting groups in the terminal positions of the oligothiophene unit.

This interesting contrast in redox behavior has been further investigated by in-situ monitoring of UV-vis absorption spectral changes while controlling the electrochemical potential applied to the polymer film cast on indium-tin oxide (ITO)-coated glass (Figure 4). As the potential applied to the polymer films was

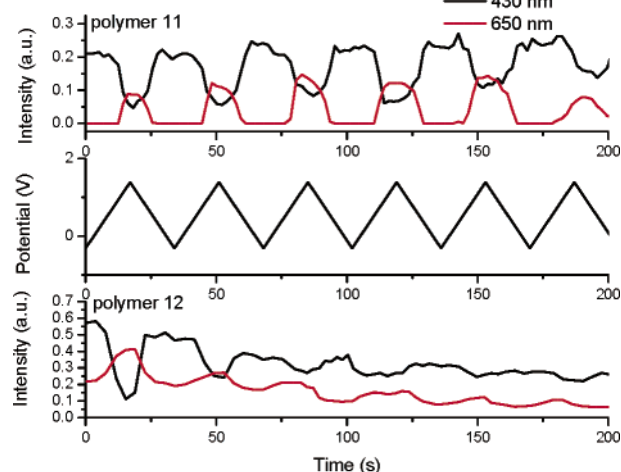


Figure 4. In-situ UV-vis absorption spectral changes monitored at 430 and 650 nm for films of polymer **11** and **12** under controlled electrochemical potential swept between -0.2 and 1.5 V. Potentials are versus the ferrocene/ferrocenium (Fc/Fc^+) couple.

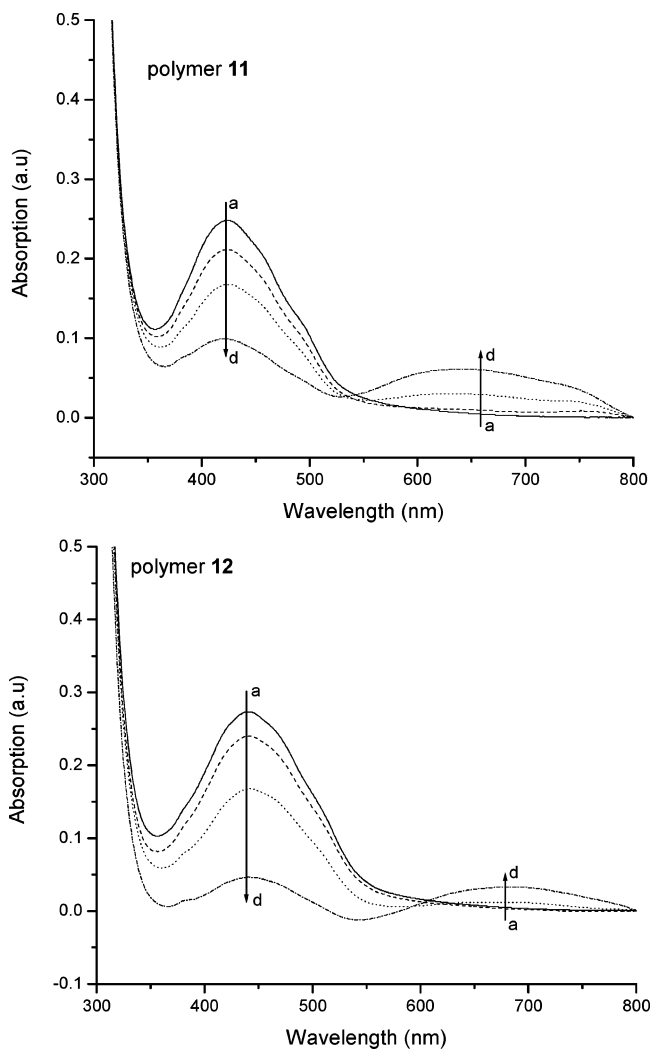


Figure 5. Spectroelectrochemical spectra for polymer **11** and **12** as a function of applied voltage in CH_3CN : (a) 0, (b) 0.7, (c) 0.8, and (d) 0.9 V.

swept linearly between -0.2 and 1.5 V (measured half-wave potential for $\text{Fc}/\text{Fc}^+ = 0.112$ V) at a scan rate of 100 mV/s, the absorption intensity monitored at 430 nm (black line, top graph in Figure 4) for polymer **11** was observed to decrease as the applied potential became more anodic (from -0.2 to 1.5 V)

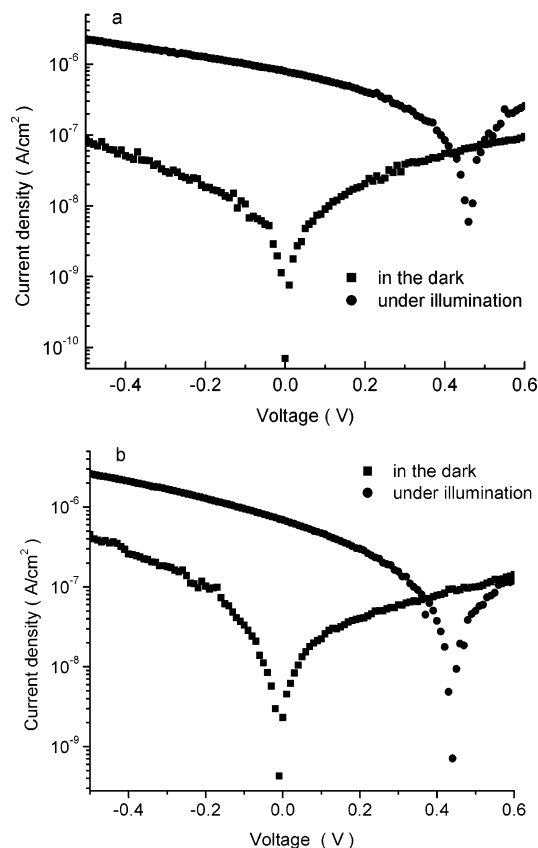


Figure 6. Current density–voltage characteristics of solar cells fabricated from polymers (a) **11** and (b) **12** in the dark and under illumination (50 mW/cm^2).

until it reached a minimum value before returning to the original level as the potential became more cathodic (from 1.5 to -0.2 V). When the absorbance at 430 nm has reached a local minimum, the corresponding intensity monitored at 650 nm has registered a local maximum peak (red line, top graph in Figure 4). The rise of the absorption peak at 650 nm may be attributed to absorption by the p-doped state of the oligothiophene side chain, and this process was more or less reversible. This reversible doping/dedoping process was accompanied by a change in the color of coated film on the ITO glass electrode between yellow (undoped state) and deep green (doped state). Further electrochemical cycling between -0.2 and 1.5 V resulted in essentially the same spectral behavior for absorption monitored at these two wavelengths for up to eight cycles, which suggests that the p-doping/dedoping process is fairly reversible for film of polymer **11**. In sharp contrast, the absorption intensity for polymer **12** monitored at 430 and 650 nm (bottom graph, Figure 4) decreased quickly just after one swept cycle, and there were little changes in intensity thereafter, indicating there was a loss in redox activity from the sexithiophene unit as a result of the initial anodic scan. This observation corroborates the redox behavior for this polymer, as depicted in Figure 3b.

The spectroelectrochemical spectra of thin films of polymers **11** and **12** in CH_3CN are also given in Figure 5. The polymer-coated ITO glass electrode was used as the working electrode, Pt as the counter electrode, and Ag/AgNO_3 as the reference electrode. As has been observed in other electrochromic polymers,¹⁶ as the voltage applied to the thin films of the polymers increased, the absorption band at $400\text{--}500 \text{ nm}$ region decreased gradually (λ_{max} : 432 nm for **11** and 441 nm for **12**) while a broad absorption band in the visible region increased continuously ($550\text{--}800 \text{ nm}$ for **11** and $600\text{--}800 \text{ nm}$ for **12**).

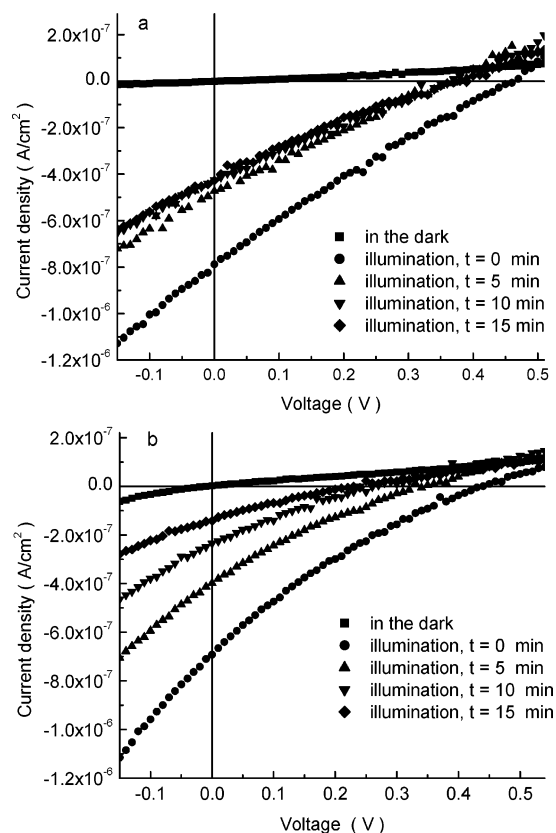


Figure 7. Current density–voltage characteristics of solar cells fabricated from polymers (a) **11** and (b) **12** in the dark and under illumination (50 mW/cm^2) measured at 5 min intervals.

During the oxidative process, the coated film on the ITO glass electrode also changed from yellow to deep green, indicating the formation of a p-doped state in the electroactive oligothiophene backbone.

Photovoltaic Properties. Single-layer photovoltaic devices with a thin layer of polymer **11** or **12** sandwiched between indium–tin oxide and thermally evaporated aluminum film (50 nm) have been fabricated. Figure 6 shows the current density–voltage characteristics of the Al/polymer/PEDOT:PSS/ITO devices in the dark and under illumination (50 mW/cm^2). Devices constructed from both polymers clearly show a rectifying behavior and exhibit significant photovoltaic effects under illumination. Our measurements indicate that these photovoltaic devices have relatively large open-circuit voltage ($V_{\text{oc}} = 0.46 \text{ V}$ for **11** and 0.43 V for **12**) and moderate short-circuit current ($I_{\text{sc}} = 0.80 \mu\text{A/cm}^2$ for **11** and $0.78 \mu\text{A/cm}^2$ for **12**). It is recognized that these single-layer polymeric solar cells still suffer from poor power conversion efficiency due to inefficient exciton dissociation, charge separation, and collection. Nevertheless, we observed that solar cells fabricated from polymer **11** consistently exhibited better device stability than that from **12** under ambient conditions (Figure 7). This point is best illustrated by repeated measurements of their device performance at 5 min intervals under operating conditions, and one notices that the current–voltage behavior of polymer **11** quickly stabilized ($t = 5, 10, 15 \text{ min}$) after the initial illumination ($t = 0 \text{ min}$). In sharp contrast, a device fabricated from polymer **12** showed a much faster and continuous decay in performance upon repeated measurements, and the lifetime is comparatively shorter compared to polymer **11**. The rather drastic difference in photovoltaic device stability together with redox behaviors suggests that it is highly desirable to prepare oligothiophene-based materials with stable end-capping units (such as phenyl

group) at the terminal positions (as in polymer **11**) for achieving good environmental stability and improved device lifetime.

Conclusion

Two structurally related new polymers **11** and **12** functionalized with conjugated oligomers in the side chain were synthesized by the ROMP method. These polymers showed interesting optical and electrochemical properties derived from the side-chain-appended oligomers as well as excellent thermal stability and film forming properties afforded by the polynorbornene backbone. The photophysical and redox behaviors of **11** and **12** are markedly different due to the different nature of the end-group substituent on the pendant oligomers. Polymer **11** with phenyl end-capped oligothiophene co-oligomer in the side chain is significantly more stable toward electrochemical oxidation compared to **12** with sexithiophene in the side chain. In-situ monitoring of the characteristic UV-vis absorption spectral changes as a function of applied electrochemical potential on polymer film unequivocally demonstrated the advantage of incorporating chemically and environmentally stable end groups on the oligothiophene unit. Polymer **11** showed a fairly reversible p-doping/dedoping process as monitored at 430 and 650 nm, while polymer **12** hardly exhibited any reversible behavior. Single-layer photovoltaic devices with **11** or **12** as the active organic layer have been fabricated and investigated. Although both devices provided relatively large open-circuit voltage and moderate short-circuit current performance, the one fabricated from **11** showed definitively better device stability than that from **12**. Tentatively, we attributed this difference in performance to the robust nature of phenyl end-capped oligothiophene co-oligomer relative to that of sexithiophene in the side chain of each polymer. Future work will focus on the improvement of power conversion efficiency and device stability for these polymers through introduction of a new electron acceptor to form a heterojunction with larger surface area and to provide continuous conduction channels for more efficient charge separation and transport.

Experimental Section

General. All chemicals were purchased from Aldrich Chemical Co. unless otherwise specified. Anhydrous *N,N*-dimethylformamide (DMF), chloroform, and acetic acid were used as received without further purification. Tetrahydrofuran (THF), dichloromethane, and diethyl ether were dried and distilled immediately prior to use. 2-(Tributylstannyl)thiophene,¹⁷ 3-(tributylstannyl)thiophene,¹⁷ 3-(5-bromopentyl)thiophene,¹⁸ and 4-(dimethylamino)pyridinium-4-toluenesulfonate (DPTS)¹⁹ were prepared according to literature procedures. 2-(Tributylstannyl)-5-phenylthiophene and 5-(tributylstannyl)-2,2'-bithiophene were prepared by following essentially the same procedure as that for 2-(tributylstannyl)thiophene.

¹H NMR and ¹³C NMR spectra were recorded on a Bruker Avance 400 FT-NMR spectrometer operating at 400 and 100 MHz, respectively. Deuterated chloroform and *d*₄-*o*-dichlorobenzene were used as the solvents. Weight-averaged molecular weight (*M*_w) and number-averaged molecular weight (*M*_n) were determined by gel permeation chromatography (GPC) using Waters Styragel HM3 and HR4 GPC columns connected in series using polystyrene as the standard and THF as the eluent. Thermogravimetric analysis (TGA) was performed on a TA Instruments (TGA 2050 thermogravimetric analyzer) module at a heating rate of 10 °C min⁻¹ under a nitrogen atmosphere. Differential scanning calorimetry (DSC) was conducted on a DSC 2920 modulated instrument at a heating rate of 10 °C min⁻¹ under a nitrogen atmosphere. The temperature regime was from room temperature to 500 °C. Polymer solution was prepared in *o*-dichlorobenzene, and polymer thin film was deposited onto glass plates by the spin-coating method. The absorption and fluorescence spectral measurements of polymer solutions and thin

films were conducted on a Shimadzu UV-2401 PC UV-vis spectrophotometer and on a Fluorolog-3 spectrofluorometer, respectively.

3-(6-(4,4-Dimethyloxazolin-2-yl)hexyl)thiophene (1). To a solution of 2,4,4-trimethyl-2-oxazoline (3.12 g, 27.6 mmol) in 100 mL of THF at -78 °C was added 11.1 mL of *n*-BuLi (2.5 M in hexanes, 27.75 mmol) under N₂. After 1 h at -78 °C, a THF solution of 3-(5-bromopentyl)thiophene (6.3 g, 27 mmol) was added over 30 min. The reaction mixture was warmed to room temperature slowly and stirred overnight. The reaction was quenched with water and was concentrated to 1/3 of the original volume. Ether was added, and the organic phase was washed with water and dried over Na₂SO₄. The crude product was purified by flash chromatography (silica gel) to afford 5.40 g (75%) of **1**. ¹H NMR (400 MHz, CDCl₃): δ 7.23–7.21 (m, 1H), 6.92–6.90 (m, 2H), 3.89 (s, 2H), 2.62 (t, 2H), 2.24 (t, 2H), 1.64–1.60 (m, 4H), 1.38–1.35 (m, 4H), 1.26 (s, 6H). ¹³C NMR (100 MHz, CDCl₃): δ 165.91, 142.91, 128.14, 124.98, 119.73, 78.77, 66.74, 30.29, 30.08, 28.84, 28.79, 28.37, 28.03, 25.89. HRMS (ESI) calcd for C₁₅H₂₃NOS: 265.1500. Found: 266.1577 [M + H]⁺.

2-Bromo-3-(6-(4,4-dimethyloxazolin-2-yl)hexyl)thiophene (2). To a solution of **1** (2.5 g, 9.43 mmol) in 45 mL of a mixture of CHCl₃/AcOH was added *N*-bromosuccinimide (NBS) (1.93 g, 10.8 mmol) in small portions at room temperature, and the resulting mixture was stirred for 12 h. The reaction mixture was poured into water and extracted with ether. The combined organic layers were washed with saturated NaHCO₃, Na₂S₂O₃, and water and dried over anhydrous Na₂SO₄. The solvent was removed in vacuo to afford 3.00 g (93%) of **2**, which was pure enough for the next step. ¹H NMR (400 MHz, CDCl₃): δ 7.17 (d, 1H), 6.77 (d, 1H), 3.89 (s, 2H), 2.55 (t, 2H), 2.24 (t, 2H), 1.62–1.57 (m, 4H), 1.37–1.34 (m, 4H), 1.26 (s, 6H). LRMS (APCI⁺) calcd for C₁₅H₂₂BrNOS: 345.06. Found: 346.0 [M + H]⁺.

3-(6-(4,4-Dimethyloxazolin-2-yl)hexyl)-2,2'-bithiophene (3). 2-(Tributylstannyl)thiophene (5.06 g, 13.5 mmol) was added to a solution of **2** (3.28 g, 9.50 mmol) in anhydrous DMF, and the resulting mixture was purged with N₂ for 30 min. A mixture of Pd(PPh₃)₂Cl₂ (200 mg, 0.28 mmol) and PPh₃ (149 mg, 0.56 mmol) was then added, and the reaction mixture was heated to 100 °C overnight. Excess DMF was removed under high vacuum, and to the residue in ethyl acetate was added 10% aqueous KF. The mixture was filtered through a pad of Celite. The filtrate was dried over Na₂SO₄ and filtered, and the solvent was removed in vacuo. The crude product was purified by flash chromatography (silica gel) to afford 2.35 g (71%) of **3**. ¹H NMR (400 MHz, CDCl₃): δ 7.30 (dd, 1H), 7.16 (d, 1H), 7.10 (dd, 1H), 7.05 (dd, 1H), 6.91 (d, 1H), 3.89 (s, 2H), 2.73 (t, 2H), 2.23 (t, 2H), 1.62–1.59 (m, 4H), 1.37–1.34 (m, 4H), 1.26 (s, 6H). ¹³C NMR (100 MHz, CDCl₃): δ 165.95, 139.41, 136.10, 130.49, 129.79, 127.27, 125.95, 125.25, 123.70, 78.82, 66.79, 30.49, 29.02, 28.94, 28.89, 28.40, 28.07, 25.91. HRMS (ESI) calcd for C₁₉H₂₅NOS₂: 347.1378. Found: 348.1446 [M + H]⁺.

3-(6-(4,4-Dimethyloxazolin-2-yl)hexyl)-5,5'-dibromo-2,2'-bithiophene (4). NBS (1.118 g, 6.28 mmol) was added, in small portions, to a solution of **3** (1.019 g, 2.94 mmol) in DMF at 0 °C. The mixture was stirred at 0 °C for 4 h and then at room temperature for 12 h. The mixture was poured into water and extracted with CH₂Cl₂. The combined organic layers were washed with saturated NaHCO₃ and water and dried over anhydrous Na₂SO₄. The solvent was removed in vacuo, and the crude product was purified by flash chromatography (silica gel) to afford 1.02 g (68%) of **4**. ¹H NMR (400 MHz, CDCl₃): δ 7.00 (d, 1H), 6.87 (s, 1H), 6.78 (d, 1H), 3.88 (s, 2H), 2.62 (t, 2H), 2.22 (t, 2H), 1.63–1.56 (m, 4H), 1.36–1.32 (m, 4H), 1.26 (s, 6H). LRMS (APCI⁺) calcd for C₁₉H₂₃Br₂NOS₂: 504.96. Found: 505.9 [M + H]⁺.

3-(6-(4,4-Dimethyloxazolin-2-yl)hexyl)-5'',5'''-diphenyl-2,2';5,2'';5',2'''-quaterthiophene (5). A solution of **4** (1.00 g, 1.98 mmol) and 2-(tributylstannyl)-5-phenylthiophene (2.22 g, 4.95 mmol) in anhydrous DMF was purged with N₂ for 30 min. A mixture of Pd(PPh₃)₂Cl₂ (70 mg, 0.10 mmol) and PPh₃ (52 mg, 0.20 mmol) was then added. The resulting mixture was heated to

100 °C overnight, cooled to room temperature, and filtered. The solvent was removed under high vacuum, and ether was added to the residue. The slurry was stirred for 30 min and filtered, and the solid was washed with ether. The solid was subsequently purified by flash chromatography (silica gel) to afford 1.00 g (76%) of **5**. ¹H NMR (400 MHz, CDCl₃): δ 7.63–7.60 (m, 4H), 7.41–7.38 (m, 4H), 7.31–7.27 (m, 2H), 7.25–7.23 (m, 2H), 7.17–7.14 (m, 3H), 7.06 (d, 1H), 7.04 (s, 1H), 3.89 (s, 2H), 2.78 (t, 2H), 2.26 (t, 2H), 1.72–1.64 (m, 4H), 1.44–1.41 (m, 4H), 1.26 (s, 6H). ¹³C NMR (100 MHz, CDCl₃): δ 165.91, 143.25, 143.17, 140.30, 137.07, 136.34, 136.29, 135.20, 134.75, 133.97, 129.40, 128.90, 127.58, 126.46, 126.37, 125.56, 124.52, 123.87, 123.78, 78.82, 66.80, 30.26, 29.37, 29.10, 28.93, 28.41, 28.10, 25.94. HRMS (ESI) calcd for C₃₉H₃₇NOS₄: 663.1758. Found: 664.1831 [M + H]⁺.

5'',5'''-Diphenyl-2,2';5,2'';5',2'''-quaterthiophene-3-heptanoic Acid (6). A mixture of **5** (520 mg, 0.783 mmol) in a mixture of 3 N HCl (60 mL) and THF (20 mL) was refluxed overnight. The heterogeneous mixture was filtered, and the solid was rinsed with water and dried to afford 473 mg (99%) of **6**. ¹H NMR (400 MHz, CDCl₃): δ 7.63–7.59 (m, 4H), 7.41–7.36 (m, 4H), 7.32–7.28 (m, 2H), 7.25 (d, 1H), 7.23 (d, 1H), 7.19–7.13 (m, 3H), 7.07–7.03 (m, 2H), 2.79 (t, 2H), 2.37 (t, 2H), 1.80–1.62 (m, 4H), 1.49–1.43 (m, 4H). LRMS (APCI) calcd for C₃₅H₃₀O₂S₄: 610.1. Found: 611.0 [M + H]⁺.

5-Norbornene-endo-2,3-bis(methylene(5'',5'''-diphenyl-2,2';5,2'';5',2'''-quaterthiophene)-3-heptanoate) (7). A mixture of **6** (440 mg, 0.72 mmol), 5-norbornene-endo-2,3-dimethanol (55 mg, 0.36 mmol), DPTS (562 mg, 1.8 mmol), and DIPC (227 mg, 1.8 mmol) in CH₂Cl₂ was refluxed overnight. The solvent was removed in vacuo, and the residual solid was purified by flash chromatography (silica gel) to afford 400 mg (83%) of **7**. ¹H NMR (400 MHz, CDCl₃): δ 7.60–7.58 (m, 8H), 7.40–7.36 (m, 8H), 7.30–7.28 (m, 4H), 7.23 (d, 2H), 7.22 (d, 2H), 7.15–7.11 (m, 6H), 7.03 (d, 2H), 7.02 (s, 2H), 6.13 (s, 2H), 3.90 (m, 2H), 3.75 (m, 2H), 2.87 (s, 2H), 2.76 (t, 4H), 2.50 (m, 2H), 2.30 (t, 4H), 1.68–1.63 (m, 8H), 1.43–1.36 (m, 10H). ¹³C NMR (100 MHz, CDCl₃): δ 173.49, 143.20, 143.12, 140.18, 137.03, 136.30, 135.35, 135.18, 134.74, 133.93, 129.45, 128.90, 127.56, 126.40, 126.34, 125.52, 124.50, 123.86, 123.78, 64.32, 48.94, 45.47, 40.60, 34.29, 30.21, 29.38, 29.13, 28.94, 24.89. LRMS (ESI) calcd for C₇₉H₇₀O₄S₈: 1338.3. Found: 1361 [M + Na]⁺. Elemental Anal. Calcd for C₇₉H₇₀O₄S₈: C, 70.81; H, 5.27. Found: C, 70.67; H, 5.07.

3-(6-(4,4-Dimethyloxazolin-2-yl)hexyl)-2,2';5,2'';5',2'''-sexithiophene (8). A solution of **4** (1.00 g, 1.98 mmol) and 5-(tributylstannyl)-2,2'-bithiophene (2.25 g, 4.95 mmol) in anhydrous DMF was purged with N₂ for 30 min. A mixture of Pd(PPh₃)₂Cl₂ (70 mg, 0.10 mmol) and PPh₃ (52 mg, 0.20 mmol) was then added. The resulting mixture was heated to 100 °C overnight, cooled to room temperature, and filtered. The solvent was removed under high vacuum, and ether was added to the residue. The slurry was stirred for 30 min and filtered, and the solid was washed with ether. The solid was subsequently purified by flash chromatography (silica gel) to afford 1.10 g (82%) of **8**. ¹H NMR (400 MHz, CDCl₃): δ 7.23–7.21 (m, 2H), 7.19–7.17 (m, 2H), 7.12 (d, 1H), 7.09–7.05 (m, 4H), 7.04–7.02 (m, 3H), 7.00 (s, 1H), 3.88 (s, 2H), 2.76 (t, 2H), 2.26 (t, 2H), 1.69–1.65 (m, 4H), 1.43–1.41 (m, 4H), 1.26 (s, 6H). ¹³C NMR (100 MHz, CDCl₃): δ 165.91, 140.33, 137.07, 137.03, 136.77, 136.32, 136.25, 135.78, 135.74, 134.89, 134.81, 129.46, 127.86, 126.50, 126.39, 124.50, 124.35, 124.23, 124.21, 123.93, 123.71, 123.66, 78.82, 66.81, 30.24, 29.36, 29.09, 28.92, 28.41, 28.09, 25.93. HRMS (ESI) calcd for C₃₅H₃₃NOS₆: 675.0886. Found: 676.0943 [M + H]⁺.

2,2';5,2'';5',2'''-Sexithiophene-3-heptanoic Acid (9). A mixture of **8** (990 mg, 1.46 mmol) in a mixture of 3 N HCl (60 mL) and THF (20 mL) was refluxed overnight. The heterogeneous mixture was filtered, and the solid was rinsed with water and dried to afford 750 mg (82%) of **9**. ¹H NMR (400 MHz, CDCl₃): δ 7.23–7.22 (m, 2H), 7.19–7.17 (m, 2H), 7.12 (d, 1H), 7.09–7.07 (m, 4H), 7.04–7.01 (m, 3H), 7.00 (s, 1H), 2.79 (t, 2H),

2.37 (t, 2H), 1.79–1.65 (m, 4H), 1.43–1.42 (m, 4H). LRMS (APCI) calcd for C₃₁H₂₆O₂S₆: 622.0. Found: 623.0 [M + H]⁺.

5-Norbornene-endo-2,3-bis(methylene(2,2';5,2'';5',2'''-sexithiophene)-3-heptanoate) (10). A mixture of **9** (647 mg, 1.04 mmol), 5-norbornene-endo-2,3-dimethanol (80 mg, 0.52 mmol), DPTS (810 mg, 2.6 mmol), and DIPC (327 mg, 2.6 mmol) in CH₂Cl₂ were refluxed overnight. The solvent was removed in vacuo, and the residual solid was purified by flash chromatography (silica gel) to afford 600 mg (85%) of **10**. ¹H NMR (400 MHz, CDCl₃): δ 7.22–7.20 (m, 4H), 7.17–7.16 (m, 4H), 7.10 (d, 2H), 7.07–7.03 (m, 8H), 7.02–7.00 (m, 6H), 6.89 (s, 2H), 6.13 (s, 2H), 3.90–3.85 (m, 2H), 3.78–3.73 (m, 2H), 2.87 (s, 2H), 2.75 (t, 4H), 2.50 (m, 2H), 2.30 (t, 4H), 1.69–1.60 (m, 8H), 1.42–1.28 (m, 10H). ¹³C NMR (100 MHz, CDCl₃): δ 173.49, 140.23, 137.05, 137.01, 136.74, 136.31, 136.23, 135.75, 135.71, 135.34, 134.89, 134.78, 129.48, 127.85, 126.45, 126.36, 124.48, 124.33, 124.21, 123.91, 123.69, 123.65, 64.32, 48.93, 45.47, 40.59, 34.28, 30.19, 29.36, 29.11, 28.91, 24.88. LRMS (ESI) calcd for C₇₁H₆₂O₄S₁₂: 1362.1. Found: 1385 [M + Na]⁺. Elemental Anal. Calcd for C₇₁H₆₂O₄S₁₂: C, 62.52; H, 4.58. Found: C, 62.66; H, 4.31.

Polymerization of Monomer 7. To a solution of **7** (195 mg, 0.146 mmol) in dry and deoxygenated CH₂Cl₂ (25 mL) was added a solution of bis(tricyclohexylphosphine)benzylideneruthenium (IV) dichloride (8 mg, 0.00972 mmol) in CH₂Cl₂ (2 mL) through a cannula. After refluxing for 22 h, during which time a precipitate had formed, excess ethyl vinyl ether was added, and the mixture was stirred for an additional 30 min. The resulting solid was filtered, washed with CH₂Cl₂, and dried to afford polymer **11** in 87% yield. ¹H NMR (400 MHz, *o*-DCB-*d*₄): δ 7.56 (br, 10H), 7.40–7.23 (m, 10H), 7.12–7.09 (m, 14H), 5.48 (br, 2H), 4.29 (br, 4H), 2.80 (br, 6H), 2.40 (br, 6H), 1.72 (br, 10H), 1.44 (br, 8H).

Polymerization of Monomer 10. To a solution of **10** (258 mg, 0.189 mmol) in dry and deoxygenated CH₂Cl₂ (20 mL) was added a solution of bis(tricyclohexylphosphine)benzylideneruthenium (IV) dichloride (7.8 mg, 0.00947 mmol) in CH₂Cl₂ (2 mL) through a cannula. After refluxing for 22 h, during which time a precipitate had formed, excess ethyl vinyl ether was added, and the mixture was stirred for an additional 30 min. The resulting solid was filtered, washed with CH₂Cl₂, and dried to afford polymer **12** in 89% yield. ¹H NMR (400 MHz, *o*-DCB-*d*₄): δ 7.15–6.96 (m, 26H), 5.50 (br, 2H), 4.29 (br, 4H), 2.78 (br, 6H), 2.41 (br, 6H), 1.72 (br, 10H), 1.44 (br, 8H).

Acknowledgment. We thank the University of Rochester, ACS PRF, and New York State Office of Science, Technology and Academic Research for financial support.

References and Notes

- (1) (a) Torsi, L.; Dodabalapur, A.; Rothberg, L. J.; Fung, A. W. P.; Katz, H. E. *Science* **1996**, *272*, 1462–1464. (b) Katz, H. E.; Bao, Z.; Gilat, S. L. *Acc. Chem. Res.* **2001**, *34*, 359–369. (c) Dimitrakopoulos, C. D.; Malenfant, P. R. L. *Adv. Mater.* **2002**, *14*, 99–117. (d) Murphy, A. R.; Liu, J.; Luscombe, C.; Kavulak, D.; Frechet, J. M. J.; Kline, R. J.; McGehee, M. D. *Chem. Mater.* **2005**, *17*, 4892–4899. (e) Facchetti, A.; Yoon, M.-H.; Marks, T. J. *Adv. Mater.* **2005**, *17*, 1705–1725. (f) Sirringhaus, H. *Adv. Mater.* **2005**, *17*, 2411–2425. (g) Zen, A.; Bilge, A.; Galbrecht, F.; Alle, R.; Meerholz, K.; Grenzer, J.; Neher, D.; Scherf, U.; Farrell, T. *J. Am. Chem. Soc.* **2006**, *128*, 3914–3915. (h) Sun, Y.; Liu, Y.; Zhu, D. *J. Mater. Chem.* **2005**, *15*, 53–65.
- (2) (a) Noma, N.; Tsuzuki, T.; Shirota, Y. *Adv. Mater.* **1995**, *7*, 647–648. (b) Roquet, S.; Cravino, A.; Leriche, P.; Aleveque, O.; Frere, P.; Roncali, J. *J. Am. Chem. Soc.* **2006**, *128*, 3459–3466. (c) Shi, C.; Yao, Y.; Yang, Y.; Pei, Q. *J. Am. Chem. Soc.* **2006**, *128*, 8980–8986. (d) Hou, J.; Tan, Z.; Yan, Y.; He, Y.; Yang, C.; Li, Y. *J. Am. Chem. Soc.* **2006**, *128*, 4911–4916. (e) Hou, J.; Tan, Z.; He, Y.; Yang, C.; Li, Y. *Macromolecules* **2006**, *39*, 4657–4662.
- (3) (a) Heeney, M.; Bailey, C.; Genevicius, K.; Shkunov, M.; Sparrowe, D.; Tierney, S.; McCulloch, I. *J. Am. Chem. Soc.* **2005**, *127*, 1078–1079. (b) McCulloch, I.; Heeney, M.; Bailey, C.; Genevicius, K.; Macdonald, I.; Shkunov, M.; Sparrowe, D.; Tierney, S.; Wagner, R.; Zhang, W.; Chabinc, M. L.; Kline, R. J.; McGehee, M. D.; Toney, M. F. *Nat. Mater.* **2006**, *5*, 328–333.

- (4) Murphy, A. R.; Liu, J.; Luscombe, C.; Kavulak, D.; Fréchet, J. M. J.; Kline, R. J.; McGehee, M. D. *Chem. Mater.* **2005**, *17*, 4892–4899.
- (5) (a) Meng, H.; Bao, Z.; Lovinger, A. J.; Wang, B.-C.; Muijsce, A. M. *J. Am. Chem. Soc.* **2001**, *123*, 9214–9215. (b) Meng, H.; Zheng, J.; Lovinger, A. J.; Wang, B.-C.; Van Patten, P. G.; Bao, Z. *Chem. Mater.* **2003**, *15*, 1778–1787.
- (6) Yoon, M.-H.; DiBenedetto, S. A.; Facchetti, A.; Marks, T. J. *J. Am. Chem. Soc.* **2005**, *127*, 1348–1349.
- (7) Videlot-Ackermann, C.; Ackermann, J.; Brisset, H.; Kawamura, K.; Yoshimoto, N.; Raynal, P.; Kassmi, A. E.; Fages, F. *J. Am. Chem. Soc.* **2005**, *127*, 16346–16347.
- (8) (a) Zhao, C.; Zhang, Y.; Wang, C.; Rothberg, L.; Ng, M.-K. *Org. Lett.* **2006**, *8*, 1585–1588.
- (9) (a) Shirota, Y. *J. Mater. Chem.* **2000**, *10*, 1–25. (b) Sivula, K.; Ball, Z. T.; Watanabe, N.; Fréchet, J. M. J. *Adv. Mater.* **2006**, *18*, 206–210.
- (10) (a) Nawa, K.; Imae, I.; Noma, N.; Shirota, Y. *Macromolecules* **1995**, *28*, 723–729. (b) Imae, I.; Nawa, K.; Ohsedo, Y.; Noma, N.; Shirota, Y. *Macromolecules* **1997**, *30*, 380–386. (c) Melucci, M.; Barbarella, G.; Zambianchi, M.; Benzi, M.; Biscarini, F.; Cavallini, M.; Bongini, A.; Fabbroni, S.; Mazzeo, M.; Anni, M.; Gigli, G. *Macromolecules* **2004**, *37*, 5692–5702. (d) Kagan, J.; Liu, H. *Synth. Met.* **1996**, *82*, 75–81. (e) Meeker, D. L.; Mudigonda, D. S. K.; Osborn, J. M.; Loveday, D. C.; Ferraris, J. P. *Macromolecules* **1998**, *31*, 2943–2946.
- (11) Ng, M.-K.; Lee, D.-C.; Yu, L. *J. Am. Chem. Soc.* **2002**, *124*, 11862–11863.
- (12) Stille, J. K. *Angew. Chem., Int. Ed. Engl.* **1986**, *25*, 508–524.
- (13) (a) Kanaoka, S.; Grubbs, R. H. *Macromolecules* **1995**, *28*, 4707–4713. (b) Schwab, P.; Grubbs, R. H.; Ziller, J. W. *J. Am. Chem. Soc.* **1996**, *118*, 100–110. (c) Weck, M.; Schwab, P.; Grubbs, R. H. *Macromolecules* **1996**, *29*, 1789–1793.
- (14) (a) Jang, S.; Sotzing, G. A.; Marquez, M. *Macromolecules* **2002**, *35*, 7293–7300. (b) Jang, S.; Marquez, M.; Sotzing, G. A. *Macromolecules* **2004**, *37*, 4351–4359.
- (15) Stepp, B. R.; Nguyen, S. T. *Macromolecules* **2004**, *37*, 8222–8229.
- (16) (a) Sankaran, B.; Reynolds, J. R. *Macromolecules* **1997**, *30*, 2582–2588. (b) Havinga, E. E.; Mutsaers, C. M. J.; Jenneskens, L. W. *Chem. Mater.* **1996**, *8*, 769–776. (c) Kumar, A.; Welsh, D. M.; Morvant, M. C.; Piroux, F.; Abboud, K. A.; Reynolds, J. R. *Chem. Mater.* **1998**, *10*, 896–902.
- (17) John, T. P.; Eric, G. R. *J. Chem. Soc., Perkin Trans. 1* **1988**, *8*, 2415–2421.
- (18) Bäuerle, P.; Würthner, F.; Heid, S. *Angew. Chem., Int. Ed. Engl.* **1990**, *29*, 419–420.
- (19) Messmore, B. W.; Hulvat, J. F.; Sone, E. D.; Stupp, S. I. *J. Am. Chem. Soc.* **2004**, *126*, 14452–14458.

MA062300S